Electroencephalography-Based Auditory Attention Decoding: Toward Neurosteered Hearing Devices

Simon Geirnaert, Servaas Vandecappelle, Emina Alickovic, Alain de Cheveigné, Edmund Lalor, Bernd Meyer, Sina Miran, Tom Francart, Alexander Bertrand

Neuro-Steered Hearing Devices

Decoding Auditory Attention From the Brain

Simon Geirnaert, Servaas Vandecappelle, Emina Alickovic, Alain de Cheveigné, Edmund Lalor, Bernd T. Meyer, Sina Miran, Tom Francart, and Alexander Bertrand

Abstract

People suffering from hearing impairment often have difficulties participating in conversations in so-called 'cocktail party' scenarios with multiple people talking simultaneously. Although advanced algorithms exist to suppress background noise in these situations, a hearing device also needs information on which of these speakers the user actually aims to attend to. Recent neuroscientific advances have shown that it is possible to determine the focus of auditory attention from non-invasive neurorecording techniques, such as electroencephalography (EEG). Based on these new insights, a multitude of auditory attention decoding (AAD) algorithms have been proposed, which could, in combination with the appropriate speaker separation algorithms and miniaturized EEG sensor devices, lead to a new generation of so-called neuro-steered hearing devices. In this paper, we address the main signal processing challenges in this field and provide a review and comparative study of state-of-the-art AAD algorithms.

I. Introduction

Current state-of-the-art hearing devices, such as hearing aids or cochlear implants, contain advanced signal processing algorithms to suppress acoustic background noise and as such assist the constantly expanding group of people suffering from hearing impairment. However, situations where multiple competing speakers are active at the same time (dubbed the 'cocktail party problem') still cause major difficulties for the hearing device user, often leading to social isolation and decreased quality of life. Beamforming algorithms that use microphone array signals to

This research is funded by an Aspirant Grant from the Research Foundation - Flanders (FWO) (for S. Geirnaert), the KU Leuven Special Research Fund C14/16/057, FWO project nr. G0A4918N, the European Research Council (ERC) under the European Unions Horizon 2020 research and innovation programme (grant agreement No 802895 and grant agreement No 637424), and the Flemish Government under the Onderzoeksprogramma Artificile Intelligentie (AI) Vlaanderen programme. The scientific responsibility is assumed by its authors.

The first two authors have implemented all the algorithms of the comparative study to ensure uniformity. All implementations have been checked and approved by at least one of the authors of the original paper in which the method was presented.

suppress acoustic background noise and extract a single speaker from a mixture lack a fundamental piece of information to assist the hearing device user in cocktail party scenarios: which speaker should be treated as the attended speaker and which other speaker(s) should be treated as the interfering noise sources? This issue is often addressed by using simple heuristics, such as look direction or speaker intensity, which often fail in practice.

Recent neuroscientific insights on how the brain synchronizes with the speech envelope [1], [2], have laid the groundwork for a new strategy to tackle this problem: extracting attention-related information directly from the origin, i.e., the brain. This is generally referred to as the auditory attention decoding (AAD) problem. In the last ten years, following these groundbreaking advances in the field of auditory neuroscience and neural engineering, the topic of AAD has gained traction in the biomedical signal processing community. In [3], a first successful AAD algorithm was proposed based on electroencephalography (EEG), which is a non-invasive, wearable, and relatively cheap neurorecording technique. The main idea is to decode the attended speech envelope from a multi-channel EEG recording using a neural decoder and to correlate the decoder output with the speech envelope of each speaker. Following this first AAD algorithm, a multitude of new AAD algorithms have been proposed [4]–[10]. These advances could, in combination with the appropriate blind speaker separation algorithms [11]–[15] and relying on rapidly evolving improvements in miniaturization and wearability of EEG sensors [16]–[19], lead to a new assistive solution for the hearing impaired: a *neuro-steered hearing device*.

Fig. 1 shows a conceptual overview of a neuro-steered hearing device. The AAD block contains an algorithm that determines the attended speaker by integrating the demixed speech envelopes and the EEG. Despite the large variety in AAD algorithms, an objective and transparent comparative study has not been performed to date, making it hard to identify which strategies are most successful. In this paper, we will briefly review various state-of-the-art AAD algorithms and provide an objective and quantitative comparative study using two independent publicly available datasets [20], [21]. To ensure fairness and correctness, this comparative study has been reviewed and endorsed by the author(s) of the original papers in which these algorithms were proposed. While the main focus of this paper is on this AAD block, we also provide an outlook on other practical challenges on the road ahead, such as the interaction of AAD with speech demixing or beamforming algorithms and challenges related to EEG sensor miniaturization.

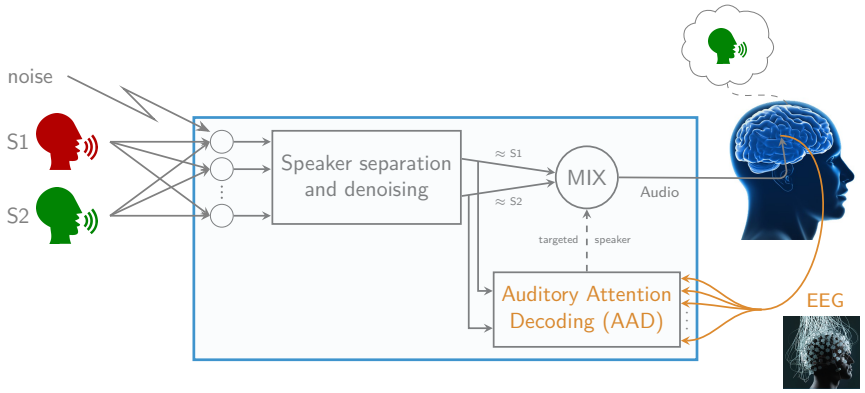

Figure 1: A conceptual overview of a neuro-steered hearing device.

II. Review of AAD algorithms

In this section, we provide a brief overview of various state-of-the-art AAD algorithms. For the sake of an easy exposition, we assume that there are only two speakers (one attended and one unattended speaker), although all algorithms can be easily generalized to more than two speakers. In the remainder of this paper, we also make abstraction of the speaker separation and denoising block in Fig. 1 and assume that the AAD block has direct access to the envelopes of the original unmixed speech sources as often done in the AAD literature. However, we will briefly return to the combination of both blocks in Section IV.

Most AAD algorithms adopt a *stimulus reconstruction* approach (also known as backward modeling or decoding). In this strategy, a multi-input single-output (MISO) neural decoder is applied to all EEG channels to reconstruct the attended speech envelope. This neural decoder is pre-trained to optimally reconstruct the attended speech envelope from the EEG data while blocking other (unrelated) neural activity. It is in this training procedure that most AAD algorithms differ. The reconstructed speech envelope is afterwards correlated with the speech envelopes of all speakers, after which the one that has the highest Pearson correlation coefficient is identified as the attended speaker (Fig. 2). This correlation coefficient is estimated over a window of τ seconds, which is referred to as the *decision window length*, corresponding to the amount of EEG data used in each decision on the attention. Typically, the AAD accuracy strongly depends on this decision window length, because the estimates of the Pearson correlation are very noisy due to the low signal-to-noise ratio of the output signal of the neural decoder.

Alternatively, the neural response in each EEG channel can be predicted from the speech envelopes via an encoder (also known as forward modeling or encoding) and can then be correlated

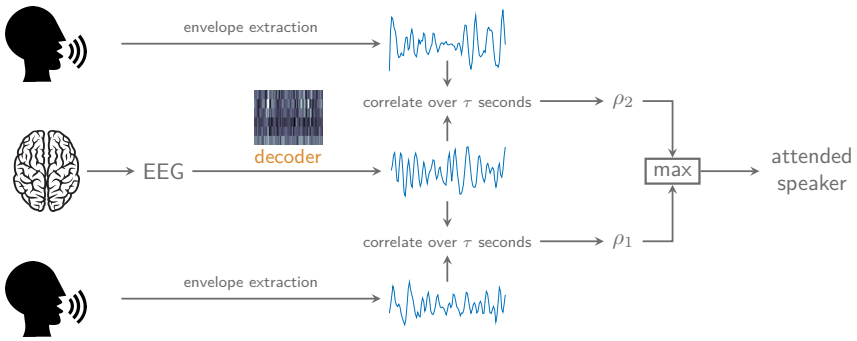

Figure 2: In the stimulus reconstruction approach, a decoder reconstructs the attended speech envelope, which is correlated with the different speech envelopes to identify the attended speaker.

with the measured EEG [5], [22]. When the encoder is linear, this corresponds to estimating impulse responses (aka temporal response functions) between the speech envelope(s) and the recorded EEG signals. For AAD, backward MISO decoding models have been demonstrated to outperform forward encoding models [5], [22], as the former can exploit the spatial coherence across the different EEG channels at its input. In this comparative study, we thus only focus on backward AAD algorithms, except for the canonical correlation analysis (CCA) algorithm (Section II-A2), which combines both a forward and backward approach.

Due to the emergence of deep learning methods, a third approach has become popular: *direct classification* [9], [10]. In this approach, the attention is directly predicted in an end-to-end fashion, without explicitly reconstructing the speech envelope.

The decoder models are typically trained in a supervised fashion, which means that the attended speaker has to be known for each data point in the training set. This requires the collection of 'ground-truth' EEG data during a dedicated experiment in which the subject is asked to pay attention to a predefined speaker in a speech mixture. The models can be trained either in a *subject-specific* fashion (based on EEG data from the actual subject under test) or in a *subject-independent* fashion (based on EEG data from other subjects than the subject under test). The latter leads to a universal (subject-independent) decoder, which has the advantage that it can be applied to new subjects without the need to go through such a tedious ground-truth EEG data collection for every new subject. However, since the brain responses of each person are different, the accuracy achieved by such universal decoders is typically lower [3]. In this paper, we only consider subject-specific decoders, which allows to achieve better accuracies, as they are tailored to the EEG of the specific end-user.

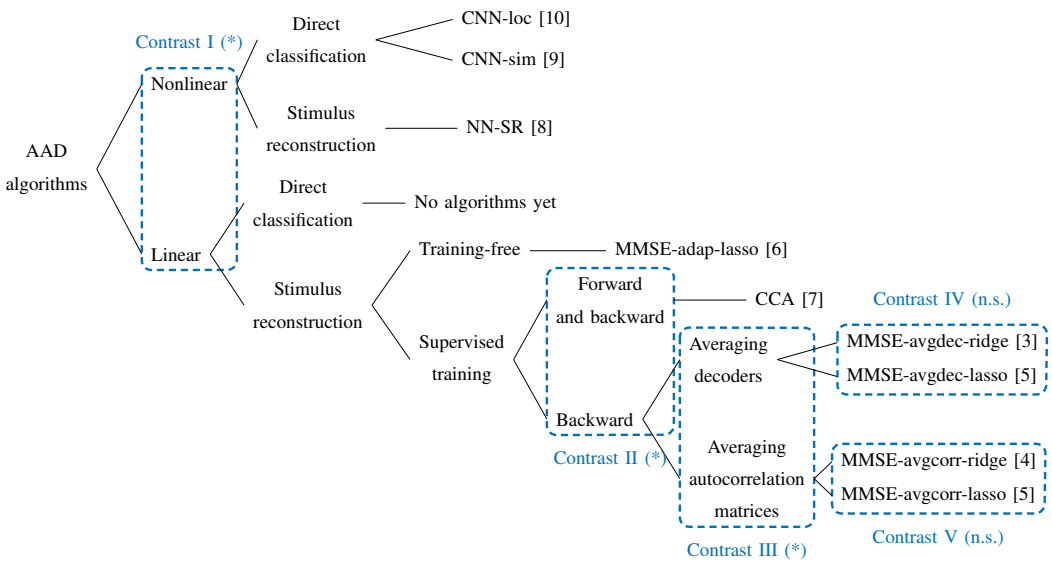

Figure 3: The included AAD algorithms in this comparative study and the planned contrasts in the statistical analysis. (*) indicates a significant difference ($p < 0.05$), (n.s.) indicates a non-significant difference.

Fig. 3 depicts a complete overview and classification of all algorithms included in our comparative study, discriminated based on their fundamental properties. In the following sections, we distinguish between linear and nonlinear algorithms.

A. Linear methods

All linear methods included in this study, which differ from each other in the features shown in the linear branch of Fig. 3, adopt the so-called stimulus reconstruction framework (Fig. 2). This boils down to applying a linear time-invariant spatio-temporal filter $D(l, c)$ on the C-channel EEG $X(t, c)$ to reconstruct the attended speech envelope $s_{\mathrm{a}}(t)$:

$$\hat{s}_{\mathrm{a}}(t) = \sum_{c=1}^{C} \sum_{l=0}^{L-1} D(l, c) X(t + l, c), \tag{1}$$

where c is the channel index, ranging from 1 to C, and l is the time lag index, ranging from 0 to $L - 1$ with L the per-channel filter length. The spatio-temporal nature of the filter is expressed through the double sum: each time sample of the speech envelope is reconstructed as a weighted sum over all channels c and over L *future* time samples of the EEG. Note that the corresponding MISO filter is anti-causal, as the brain responds to the stimulus, such that only future EEG time samples can be used to predict the current stimulus sample.

Eq. (1) can be rewritten as $\hat{s}_{\mathrm{a}}(t) = \mathbf{d}^{\mathrm{T}}\mathbf{x}(t)$, using $\mathbf{d} \in \mathbb{R}^{LC\times 1}$, collecting all decoder coefficients for all time lags and channels, and $\mathbf{x}(t) = \begin{bmatrix}\underline{\mathbf{x}}_1(t)^{\mathrm{T}} & \underline{\mathbf{x}}_2(t)^{\mathrm{T}} & \cdots & \underline{\mathbf{x}}_C(t)^{\mathrm{T}}\end{bmatrix}^{\mathrm{T}} \in \mathbb{R}^{LC\times 1}$, with $\mathbf{x}_c(t) = \begin{bmatrix}x_c(t) & x_c(t+1) & \cdots & x_c(t+L-1)\end{bmatrix}^{\mathrm{T}}$ (the same indexing holds for the decoder $\mathbf{d}$).

1) Supervised minimum mean squared error backward modeling (MMSE): The most basic way of training the decoder, first presented in the AAD-context in [3], is by minimizing the mean-square error (MSE) between the actual attended envelope and the reconstructed attended envelope. Using sample estimates, assuming that there are T samples available, the MMSE-based formulation becomes equivalent to the least-squares (LS) formulation:

$$\hat{\mathbf{d}} = \underset{\mathbf{d}}{\operatorname{argmin}} \left|\left|\mathbf{s}_{\mathrm{a}} - \mathbf{X}\mathbf{d}\right|\right|_2^2, \tag{2}$$

with $\mathbf{X} = \begin{bmatrix}\mathbf{x}(0) & \cdots & \mathbf{x}(T-1)\end{bmatrix}^{\mathrm{T}} \in \mathbb{R}^{T\times LC}$ and $\mathbf{s}_{\mathrm{a}} = \begin{bmatrix}s_{\mathrm{a}}(0) & \cdots & s_{\mathrm{a}}(T-1)\end{bmatrix}^{\mathrm{T}} \in \mathbb{R}^{T\times 1}$. The normal equations lead to the solution $\hat{\mathbf{d}} = (\mathbf{X}^{\mathrm{T}}\mathbf{X})^{-1}\mathbf{X}^{\mathrm{T}}\mathbf{s}_{\mathrm{a}}$. The first factor corresponds to an estimation of the autocorrelation matrix $\hat{\mathbf{R}}_{xx} = \frac{1}{T}\sum_{t=0}^{T-1}\mathbf{x}(t)\mathbf{x}(t)^{\mathrm{T}} \in \mathbb{R}^{LC\times LC}$, while the second factor corresponds to the cross-correlation vector $\hat{\mathbf{r}}_{xs_{\mathrm{a}}} = \frac{1}{T}\sum_{t=0}^{T-1}\mathbf{x}(t)s_{\mathrm{a}}(t) \in \mathbb{R}^{LC\times 1}$. Note that minimizing the MSE is equivalent to maximizing the Pearson correlation coefficient between the reconstructed and attended speech envelope [4].

To avoid overfitting, two types of regularization are used in AAD literature: ridge regression/L_2-norm regularization and L_1-norm/sparse regularization, also known as the least absolute shrinkage and selection operator (lasso). In the former, (2) becomes:

$$\hat{\mathbf{d}} = \underset{\mathbf{d}}{\operatorname{argmin}} \left|\left|\mathbf{s}_{\mathrm{a}} - \mathbf{X}\mathbf{d}\right|\right|_2^2 + \lambda z \left|\left|\mathbf{d}\right|\right|_2^2 \Rightarrow \hat{\mathbf{d}} = (\mathbf{X}^{\mathrm{T}}\mathbf{X} + \lambda z\mathbf{I})^{-1}\mathbf{X}^{\mathrm{T}}\mathbf{s}_{\mathrm{a}}, \tag{3}$$

with $\mathbf{I} \in \mathbb{R}^{LC\times LC}$ the unit matrix, and where the regularization hyperparameter λ is defined relative to $z = \frac{\mathrm{trace}(\mathbf{X}^{\mathrm{T}}\mathbf{X})}{LC}$. In the latter, (2) becomes:

$$\hat{\mathbf{d}} = \underset{\mathbf{d}}{\operatorname{argmin}} \left|\left|\mathbf{s}_{\mathrm{a}} - \mathbf{X}\mathbf{d}\right|\right|_2^2 + \lambda q \left|\left|\mathbf{d}\right|\right|_1, \tag{4}$$

where the regularization hyperparameter λ is now defined relative to $q = ||\mathbf{X}^{\mathrm{T}}\mathbf{s}_{\mathrm{a}}||_\infty$, which is defined as the L_∞-norm (largest absolute value) of the cross-correlation vector $\mathbf{X}^{\mathrm{T}}\mathbf{s}_{\mathrm{a}}$. Similar to [5], we here use the alternating direction method of multipliers (ADMM) to iteratively obtain the solution of (4). The optimal value λ can be found using a cross-validation scheme. Other regularization methods, such as Tikhonov regularization, have been proposed as well [22].

Assume a given training set consisting of K segments of data of a specific length T. These segments can either be constructed artificially by segmenting a continuous recording (usually for the sake of cross-validation), or they can correspond to different experimental trials (potentially

Method	**Cost function**	**Solution**
Ridge regression + averaging of decoders [3] (MMSE-avgdec-ridge)	$\hat{\mathbf{d}}_k = \underset{\mathbf{d}}{\operatorname{argmin}} \, \|\|\mathbf{s}_{\mathrm{a}_k} - \mathbf{X}_k\mathbf{d}\|\|_2^2 + \lambda z_k \, \|\|\mathbf{d}\|\|_2^2$	$\hat{\mathbf{d}}_k = (\mathbf{X}_k^{\mathrm{T}}\mathbf{X}_k + \lambda z_k \mathbf{I})^{-1}\mathbf{X}_k^{\mathrm{T}}\mathbf{s}_{\mathrm{a}_k}$ and $\hat{\mathbf{d}} = \frac{1}{K}\sum_{k=1}^{K}\hat{\mathbf{d}}_k$
Lasso + averaging of decoders [5] (MMSE-avgdec-lasso)	$\hat{\mathbf{d}}_k = \underset{\mathbf{d}}{\operatorname{argmin}} \, \|\|\mathbf{s}_{\mathrm{a}_k} - \mathbf{X}_k\mathbf{d}\|\|_2^2 + \lambda q_k \, \|\|\mathbf{d}\|\|_1$	ADMM and $\hat{\mathbf{d}} = \frac{1}{K}\sum_{k=1}^{K}\hat{\mathbf{d}}_k$
Ridge regression + averaging of correlation matrices [4] (MMSE-avgcorr-ridge)	$\hat{\mathbf{d}} = \underset{\mathbf{d}}{\operatorname{argmin}} \sum_{k=1}^{K} \|\|\mathbf{s}_{\mathrm{a}_k} - \mathbf{X}_k\mathbf{d}\|\|_2^2 + \lambda z \, \|\|\mathbf{d}\|\|_2^2$	$\hat{\mathbf{d}} = \left(\sum_{k=1}^{K}\mathbf{X}_k^{\mathrm{T}}\mathbf{X}_k + \lambda z\mathbf{I}\right)^{-1}\sum_{k=1}^{K}\mathbf{X}_k^{\mathrm{T}}\mathbf{s}_{\mathrm{a}_k}$
Lasso + averaging of correlation matrices [5] (MMSE-avgcorr-lasso)	$\hat{\mathbf{d}} = \underset{\mathbf{d}}{\operatorname{argmin}} \sum_{k=1}^{K} \|\|\mathbf{s}_{\mathrm{a}_k} - \mathbf{X}_k\mathbf{d}\|\|_2^2 + \lambda q \, \|\|\mathbf{d}\|\|_1$	ADMM

Table I: A summary of the four supervised backward AAD algorithms.

from different subjects, e.g., when training a subject-independent decoder). There exist various flavors of combining these different segments in the process of training a decoder. As suggested in the seminal paper of [3], decoders $\mathbf{d}_k$ can be trained per segment k, after which all decoders are averaged to obtain a single, final decoder $\mathbf{d}$. In [4], an alternative scheme is proposed, where, instead of estimating a decoder per segment separately, the loss function (3) or (4) is minimized over all K segments at once. As can be seen from the solution in Table I, this is equivalent to first estimating the autocorrelation matrix and cross-correlation vector via averaging the sample estimates per segment, whereafter one decoder is computed. It is easy to see that this is mathematically equivalent to concatenating all the data in one big matrix $\mathbf{X} \in \mathbb{R}^{KT \times LC}$ and vector $\mathbf{s}_{\mathrm{a}} \in \mathbb{R}^{KT \times 1}$ and computing the decoder straightforwardly. As such, it is an example of the *early integration* paradigm, versus *late integration* in the former case when averaging K separate decoders. Both versions are included in our comparative study.

Table I shows the four different flavors of the MMSE/LS-based decoder that were proposed as different AAD algorithms in [3]–[5], adopting different regularization techniques (L_2/L_1-regularization) or ways to train the decoder (averaging decoders or correlation matrices).

2) Canonical correlation analysis (CCA): CCA to decode the auditory brain has been proposed in [7], [23]. It has been applied to the AAD problem for the first time in [5]. CCA combines a

spatio-temporal backward (decoding) model $\mathbf{w}_x \in \mathbb{R}^{LC\times 1}$ on the EEG and a temporal forward (encoding) model $\mathbf{w}_{s_\mathrm{a}} \in \mathbb{R}^{L_\mathrm{a}\times 1}$ on the speech envelope, with L_a the number of filter taps of the encoding filter. In this sense, CCA differs from the previous approaches, which were all different flavors of the same MMSE/LS-based decoder. In CCA, both the forward and backward model are estimated *jointly* such that their outputs are maximally correlated:

$$\max_{\mathbf{w}_x,\mathbf{w}_{s_\mathrm{a}}} \frac{\mathbb{E}\left\{\left(\mathbf{w}_x^\mathrm{T}\mathbf{x}(t)\right)\left(\mathbf{w}_{s_\mathrm{a}}^\mathrm{T}\mathbf{s}_\mathrm{a}(t)\right)\right\}}{\sqrt{\mathbb{E}\left\{\left(\mathbf{w}_x^\mathrm{T}\mathbf{x}(t)\right)^2\right\}}\sqrt{\mathbb{E}\left\{\left(\mathbf{w}_{s_\mathrm{a}}^\mathrm{T}\mathbf{s}_\mathrm{a}(t)\right)^2\right\}}} = \max_{\mathbf{w}_x,\mathbf{w}_{s_\mathrm{a}}} \frac{\mathbf{w}_x^\mathrm{T}\mathbf{R}_{xs_\mathrm{a}}\mathbf{w}_{s_\mathrm{a}}}{\sqrt{\mathbf{w}_x^\mathrm{T}\mathbf{R}_{xx}\mathbf{w}_x}\sqrt{\mathbf{w}_{s_\mathrm{a}}^\mathrm{T}\mathbf{R}_{s_\mathrm{a}s_\mathrm{a}}\mathbf{w}_{s_\mathrm{a}}}}, \tag{5}$$

where $\mathbf{s}_\mathrm{a}(t) = \begin{bmatrix} s_\mathrm{a}(t) & s_\mathrm{a}(t-1) & \cdots & s_\mathrm{a}(t-L_\mathrm{a}+1)\end{bmatrix}^\mathrm{T} \in \mathbb{R}^{L_\mathrm{a}\times 1}$. Note that the audio filter $\mathbf{w}_{s_\mathrm{a}}$ is a causal filter (as opposed to the EEG filter $\mathbf{w}_x$), as the stimulus precedes the brain response. The solution of the optimization problem in (5) can be easily retrieved by solving a generalized eigenvalue decomposition (details in [4], [5]).

In CCA, the backward model $\mathbf{w}_x$ and forward model $\mathbf{w}_{s_\mathrm{a}}$ are extended to a set of J filters $\mathbf{W}_x \in \mathbb{R}^{LC\times J}$ and $\mathbf{W}_{s_\mathrm{a}} \in \mathbb{R}^{L_\mathrm{a}\times J}$ for which the outputs are maximally correlated, but mutually uncorrelated (the J outputs of $\mathbf{W}_x^\mathrm{T}\mathbf{x}(t)$ are uncorrelated to each other and the J outputs of $\mathbf{W}_{s_\mathrm{a}}^\mathrm{T}\mathbf{s}_\mathrm{a}(t)$ are uncorrelated to each other). There are now thus J Pearson correlation coefficients between the outputs of the J backward and forward filters (aka canonical correlation coefficients), which are collected in the vector $\boldsymbol{\rho}_i \in \mathbb{R}^{J\times 1}$ for speaker i, whereas before, there was only one per speaker. Furthermore, because of the way CCA constructs the filters, it can be expected that the first components are more important than the later ones. To find the optimal way of combining the canonical correlation coefficients, a linear discriminant analysis (LDA) classifier can be trained, as proposed in [7]. To generalize the maximization of the correlation coefficients of the previous AAD algorithms (which is equivalent to taking the sign of the difference of the correlation coefficients of both speakers), we propose here to construct a feature vector $\mathbf{f} \in \mathbb{R}^{J\times 1}$ by subtracting the canonical correlation vectors: $\mathbf{f} = \boldsymbol{\rho}_1 - \boldsymbol{\rho}_2$, and classify $\mathbf{f}$ with an LDA classifier. As proposed in [7], PCA is being used as a preprocessing step on the EEG, to reduce the number of parameters. In fact, this is a way of regularizing CCA and can as such be viewed as an alternative to the regularization techniques proposed in other methods.

3) Training-free MMSE-based with lasso (MMSE-adap-lasso): In [6], a fundamentally different AAD algorithm is proposed. All other AAD algorithms in this comparative study are *supervised*, batch-trained algorithms, which have a separate training and testing stage. First, the decoders need to be trained in a supervised manner using a large amount of ground-truth data, after which they can be applied to new test data. In practice, this necessitates a (potentially

cumbersome) a priori training stage, resulting in a fixed decoder, which does not adapt to the non-stationary EEG signal characteristics, e.g., due to changing conditions or brain processes. The AAD algorithm in [6] aims to overcome these issues by adaptively estimating a decoder for each speaker and simultaneously using the outputs to decode attention. Therefore, this training-free AAD algorithm has the advantage of adapting the decoders to non-stationary signal characteristics, however, without requiring the same, large amount of ground-truth data as the supervised AAD algorithms.

In this comparative study, we have removed the state-space and dynamic decoder estimation modules to produce a single decision for each decision window, similar to other AAD algorithms (the full description of the algorithm can be found in [6]). This leads to the following formulation:

$$\hat{\mathbf{d}}_{i,l} = \underset{\mathbf{d}}{\operatorname{argmin}} \left|\left|\mathbf{s}_{i,l} - \mathbf{X}_l\mathbf{d}\right|\right|_2^2 + \lambda q \left|\left|\mathbf{d}\right|\right|_1 , \tag{6}$$

for the i^{th} speaker in the l^{th} decision window. In the context of AAD, for every new incoming window of τ seconds of EEG and audio data, two decoders are thus estimated (one for each speaker). As an attentional marker, these estimated decoders could be applied to the EEG data $\mathbf{X}_l$ of the l^{th} decision window to compute the correlation with their corresponding stimuli envelopes. In addition, the authors of [6] propose to identify the attended speaker by selecting the speaker with the largest L_1-norm of its corresponding decoder $\hat{\mathbf{d}}_{i,l}$, as the attended decoder should exhibit more sparse, significant peaks, while the unattended decoder should have smaller, randomly distributed coefficients. The regularization parameter is again being cross-validated and defined in the same way as for MMSE-avgdec/corr-lasso. To prevent overfitting by decreasing the number of parameters to be estimated, the authors of [6] have proposed to a priori select a subset of EEG channels. In our comparative study, we also adopt this approach and select the same channels.

B. Nonlinear methods

Nonlinear methods based on (deep) neural networks can also adopt a stimulus reconstruction approach [8], similar to the linear methods, but can also classify the attended speaker directly from the EEG and the audio (aka direct classification) [9], [10]. However, these nonlinear methods are known to be more vulnerable to overfitting [10], in particular for the small-size datasets that are typically collected in AAD research. In order to appreciate the differences between current neural network-based AAD approaches, we only give a concise description of each architecture, and we refer to the respective papers for further details.

1) Fully connected stimulus reconstruction neural network (NN-SR): In [8], the authors proposed a fully-connected neural network with a single hidden layer that reconstructs the envelope based on a segment of EEG. Their input layer consists of LC neurons (similar to a linear decoder), with L the number of time lags and C the number of EEG channels. These neurons are connected to a hidden layer with two neurons and a $\tanh$ activation function. These two neurons are then finally combined into a single output neuron that uses a linear activation function and which outputs one sample of the reconstructed envelope.

The network is trained to minimize $1-\rho(\hat{\mathbf{s}}_\mathrm{a}, \mathbf{s}_\mathrm{a})$ over a segment of M training samples (within this segment the neural network coefficients are kept constant), with $\rho(\cdot)$ the Pearson correlation coefficient, and $\hat{\mathbf{s}}_\mathrm{a}, \mathbf{s}_\mathrm{a} \in \mathbb{R}^{M\times 1}$ the reconstructed and attended envelope, respectively. Minimizing this cost function is equivalent to maximizing the Pearson correlation coefficient between the reconstructed and attended speech envelope, similar to linear stimulus reconstruction approaches. The trained network is then used as a decoder, where the speech envelope showing the highest correlation with the decoder output is selected as the attended speaker.

2) Convolutional neural network to compute similarity between EEG and stimulus (CNN-sim): In [9], a CNN is proposed to directly compare a $C \times T$ EEG segment with a $1 \times T$ speech envelope. This network is trained to output a similarity score between the EEG and the speech envelope using a binary cross-entropy cost function. The speech envelope that, according to the trained CNN, is most similar to the EEG, is then identified as the attended speaker. Compared to CNN-loc, this network is deeper, consisting of two convolutional layers instead of one, and four fully connected layers instead of two (combined with batch normalization and dropout). An exponential linear unit is here used as a nonlinear activation function. Details about the training, which is performed both on attended *and* unattended speech envelopes, can be found in [9].

3) Convolutional neural network to determine spatial locus of attention (CNN-loc): In [10], a convolutional neural network (CNN) is proposed to determine the spatial locus of attention (i.e., the directional focus of attention, e.g., left or right), solely based on the EEG. This is thus a fundamentally different approach to tackle the AAD problem, which has the advantage of not requiring the individual speech envelopes (see also Section IV). Furthermore, it avoids the requirement to estimate a correlation coefficient over a relatively long decision window length as in all aforementioned algorithms, thereby avoiding large algorithmic delays.

This CNN determines the spatial locus of attention, starting from a $C \times T$ EEG segment. The first convolutional layer consists of five spatio-temporal filters, with lags L similar to before,

each outputting a one-dimensional time series of length T, on which a rectifying linear unit (ReLu) activation function is applied. Afterwards, an average pooling layer is used to condense each output series into a scalar, leading to a five-dimensional vector. This vector is then used as an input for two fully connected layers, the first one consisting of five neurons with a sigmoid activation function, the output layer consisting of two neurons and a softmax layer.

A cross-entropy cost function is minimized using mini-batch gradient descent. Weight decay regularization is applied, as well as a post-training selection of the optimal model based on the validation loss. Furthermore, during training, not only data from the subject under test (as in all other methods) but also data from other subjects are used, as it was found in [10] that this prevents the model from overfitting on the training data in case only a limited amount data of the subject under test is available. Therefore, this inclusion of data from other subjects can be seen as a type of regularization.

III. Comparative study of AAD algorithms

We compared the aforementioned state-of-the-art AAD algorithms on two publicly available datasets [20], [21] in a subject-specific manner. Both datasets have been collected with the purpose of AAD, using a competing talker setup in which two stories are simultaneously narrated. Details on the datasets and the preprocessing of the EEG and audio data are described in **[Pop-out box 1]**. Note that all algorithms, including the deep learning methods, are re-trained from scratch on each dataset separately.

Given a decision window length τ, the performance of each algorithm is evaluated via the accuracy $p \in [0, 100]\%$, defined as the percentage of correctly classified decision windows. Since EEG is the superimposed activity of many different (neural) processes, the correlation ρ between the reconstructed and attended envelope is typically quite low (in the order of 0.05-0.2). Therefore, it is important to use a sufficiently long decision window such that the decision process is less affected by estimation noise in ρ due to the finite sample size. As a result, the accuracy p generally increases for longer decision window lengths τ, leading to a so-called '$p(\tau)$-performance curve'. These accuracies are obtained using the cross-validation procedure described in **[Pop-outbox 2]**.

This $p(\tau)$-performance curve thus presents a trade-off between accuracy and decision delay of the AAD system (a long decision length implies a slower reaction time to a switch in attention). In [24], the *minimal expected switch duration* (MESD) metric has been proposed to resolve this trade-off in order to more easily compare AAD algorithms. The MESD metric determines the most optimal point on the $p(\tau)$-performance curve in the context of attention-steered gain control

by minimizing the expected time it takes to switch the gain between two speakers in an optimized robust gain control system. As such, it outputs a single-number time metric (the MESD [s]) for a $p(\tau)$-performance curve and thus removes the loss of statistical power due to multiple-comparison corrections in statistical hypothesis testing (due to testing for multiple decision window lengths). Furthermore, the MESD ensures that the statistical comparison is automatically focused on the most practically relevant points on the $p(\tau)$-performance curve, which typically turn out to be the ones corresponding to short decision window lengths $\tau < 10\,\mathrm{s}$ [24]. Note that a higher MESD corresponds to a worse AAD performance and vice versa.

A. Statistical analysis

To statistically compare the included AAD algorithms, we adopt a linear mixed-effects model (LMM) on the MESD values with the AAD algorithm as a fixed effect and with subjects as a repeated-measure random effect. Five contrasts of interest were set a priori according to the binary tree structure in Fig. 3. Algorithms that did not perform significantly better than chance are excluded from the statistical analysis, which is why some algorithms are not included in the contrasts (see Section III-B1). The planned contrasts reflect the most important different features between AAD algorithms, as shown in Fig. 3, motivating the way they are set. The significance level is set at $\alpha = 0.05$.

B. Results

1) Performance curves: Fig. 4 shows the $p(\tau)$-performance curves of the different AAD algorithms on both datasets. For the MMSE-based decoders, it is observed that there barely is an effect of the type of regularization, and that averaging correlation matrices (early integration) consistently outperforms averaging decoders (late integration). Furthermore, CCA outperforms all other linear algorithms. Lastly, on Das-2015, it is clear that decoding the spatial locus of attention using CNN-loc substantially outperforms the stimulus reconstruction methods for short decision windows ($< 10\,\mathrm{s}$), where CNN-loc appears to be less affected by the decision window length. However, the standard error on the mean is much higher for the CNN-loc algorithm than for the other methods, indicating a higher inter-subject variability.

The performances of MMSE-adap-lasso, CNN-sim, and NN-SR are not shown in Fig. 4 as they did not exceed the significance level on either of the two datasets. As these algorithms did not significantly outperform a random classifier, they were excluded from the statistical analysis.

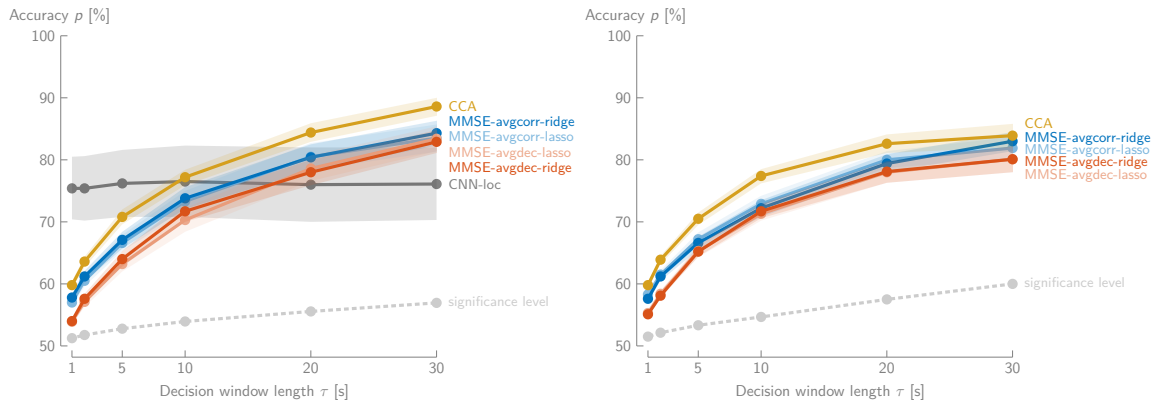

(a) (b)

Figure 4: The accuracy p (mean $\pm$ standard error on the mean across subjects) as a function of the decision window length τ for (a) Das-2015 and (b) Fuglsang-2018. MMSE-adap-lasso, CNN-sim, and NN-SR did not perform significantly better than a random classifier and are not depicted. CNN-loc only exceeded the significance level on Das-2015.

Furthermore, CNN-loc also did not perform better than chance level on Fuglsang-2018. As such, planned contrast I is also excluded from the analysis for Fuglsang-2018.

2) Subject-specific MESD performance: A visual analysis of the per-subject MESD values (Fig. 5) confirms the trends based on the performance curves. These trends are also confirmed by the statistical analysis[1] using the LMM. There indeed is a significant improvement when decoding the spatial locus of attention via a nonlinear method and the linear stimulus reconstruction methods ($p < 0.001$ (Das-2015)). Furthermore, CCA significantly outperforms all backward stimulus reconstruction decoders ($p < 0.001$ (Das-2015), $p < 0.001$ (Fuglsang-2018)), while there is also a significant improvement when averaging correlation matrices compared to averaging decoders ($p = 0.0028$ (Das-2015), $p < 0.001$ (Fuglsang-2018)). There is no significant effect of the specific regularization technique ($p = 0.79$ (Das-2015), $p = 0.30$ (Fuglsang-2018) in averaging correlation matrices; $p = 0.57$ (Das-2015), $p = 0.91$ (Fuglsang-2018) in averaging decoders).

C. Discussion

From the results and statistical analysis, it is clear that CCA [7], which adopts a joint forward and backward model, outperforms the other stimulus reconstruction methods. Furthermore, the

[1]The two outlying subjects of the CNN-loc algorithm were removed in all comparisons on the Das-2015 dataset.

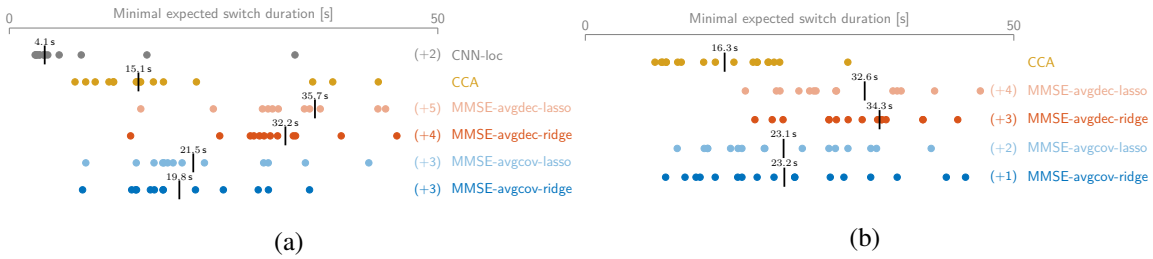

Figure 5: The per subject MESD values, with the median indicated with a bar, for (a) Das-2015 and (b) Fuglsang-2018. The number of data points with an MESD $> 50\,\mathrm{s}$ are indicated as (+x). However, these were included in the computation of the medians.

CNN-loc method [10], which decodes the spatial locus of attention based on the EEG alone (i.e., without using the speech stimuli), substantially outperforms all stimulus reconstruction methods on the Das-2015 dataset at short decision window lengths, leading to substantially lower MESDs. This relatively high performance at short decision windows is attributed to the fact that this method avoids correlating the decoded EEG with the speech envelope, thereby not suffering from the noise-susceptible correlation estimation. However, the non-significant performance of CNN-loc on the Fuglsang-2018 dataset implies that alternative algorithms for decoding the spatial locus of attention might be required to improve robustness and generalization in different conditions.

Remarkably, while the traditional linear stimulus reconstruction methods are found to perform well across datasets, none of the nonlinear (neural network) methods achieve a significant performance on *both* benchmark datasets, even though high performances were obtained on the respective datasets used in [8]–[10]. This shows that these architectures do not always generalize well, even after re-training them on a new dataset (note that the implementations in our benchmark study were validated by the original authors to rule out potential discrepancies in the implementation). Due to the black-box nature of these methods, it remains unclear what causes success on one dataset and failure on another. One possible explanation is that the design process that eventually led to the reported network architecture was too tailored to a particular dataset, despite proper cross-validation. Furthermore, (deep) neural networks may potentially pick up subtle patterns that may change or become absent in different experimental set-ups due to differences in equipment, speech stimuli, or experiment protocols.

Although this lack of reproducibility across datasets seems to undermine the practical usage of the presented nonlinear methods for AAD, they should not be immediately discarded. The

current benchmark datasets are possibly too small for these methods to draw firm conclusions. AAD based on (deep) neural networks may become more robust when larger datasets become available, containing more subjects, more EEG data per subject, and more variation in experimental conditions. Nevertheless, the results of this comparative study point out the risks of overfitting and overdesigning these architectures, thereby emphasizing the importance of extensive validation with multiple datasets.

IV. Open challenges and outlook

A. Effects of speaker separation and denoising algorithms

As explained in Section II, most AAD algorithms require access to the speech envelopes of the individual speakers. However, in the context of neuro-steered hearing devices, this would require the extraction of these per-speaker envelopes from the hearing aid's microphone recordings. It is expected that the performed speaker separation is not perfect, affecting the quality of the speech envelopes, and thus also affecting the AAD algorithms that use these envelopes. Correspondingly, AAD algorithms that do not rely on this speaker separation step, such as decoding the spatial locus of attention [10], have an inherent major advantage. In any case, a speech enhancement algorithm is required to eventually extract the attended speaker, for which advanced and well-performing signal processing algorithms exist (e.g., [25]–[27]).

A few studies have already combined AAD with speaker separation and denoising algorithms, both using traditional beamforming approaches [11], [15], [28], and deep neural networks for speaker separation [12], [13], [28]. Remarkably, many of these studies show only minor or hardly any effects on the AAD performance when using the demixed speech signals, even in challenging noisy conditions [15], [28], and despite significant distortions on the envelopes. These positive results are paramount for the practical applicability of neuro-steered hearing devices.

Finally, instead of treating the speaker extraction and AAD as two separate problems (as is the case in all aforementioned studies), one could also aim to solve both problems simultaneously. In [14], the speaker extraction and AAD problem are coupled together in a joint optimization problem, where the beamformer is enforced to generate an output signal that is correlated to the output of a backward MMSE neural decoder.

B. EEG miniaturization and wearability effects

The data used in this paper are recorded using expensive, heavy, and bulky EEG recording systems. The realization of neuro-steered hearing devices requires a wearable, concealable EEG

monitoring system. The research towards such concealable EEG systems is very active, resulting in novel devices that acquire the EEG for example in the ear (e.g., [17]) or around the ear (e.g., [16]). Such wearable, concealable EEG systems, however, provide only a limited amount of EEG channels, which only record brain activity within a small area. A first analysis using such an around-the-ear EEG system in the context of AAD showed potential, albeit with a significant decrease in performance [18].

In another (top-down) approach, the optimal number and location of miniaturized EEG sensors (combined in nodes) are determined in the context of AAD [19]. It was shown that using a data-driven selection of the best 10 EEG channels of a standard 64-channel EEG cap does not reduce the AAD performance. Moreover, in the same work, it was also demonstrated that using EEG measured by mini-EEG devices with electrodes separated by short distances, results in similar performances to EEG measured using long-distance EEG montages, when these mini-EEG devices are positioned strategically on the scalp.

C. Outlook

Several studies have demonstrated that it is possible to decode the auditory attention from a non-invasive neurorecording technique such as EEG. In our comparative study, we have shown that most of these results are reproducible on different data sets. However, even for the best linear (stimulus reconstruction) method (CCA), the accuracy at short decision windows is still too low, potentially leading to too slow reactions of the system to shifts in auditory attention, as indicated by a median MESD of $15\,\mathrm{s}$. The results of this study have demonstrated that an alternative strategy, such as decoding the spatial locus of attention, could significantly improve on these short decision window lengths. Although nonlinear (deep learning) methods are believed to be able to substantially improve AAD performances, our study has demonstrated that the reported results obtained by these methods are hard to replicate on multiple independent AAD datasets. A major future challenge for AAD research is the design of an algorithm or strategy that reliably improves on short decision windows, and which is reproducible on different independent datasets.

Furthermore, most of the presented AAD algorithms require supervised training and are fixed during operation. To avoid cumbersome a priori training sessions for each individual user, as well as to adapt to the time-varying statistics of the EEG (e.g., in different listening scenarios), training-free or unsupervised adaptive AAD algorithms should be developed. While several steps have been made in that direction [6], the results of this study show that we are still far away from a practical solution.

Furthermore, these AAD algorithms need to be further evaluated in real-life situations, taking various realistic listening scenarios into account, as well as on potential hearing device users [29]. The individual building blocks of a neuro-steered hearing device (Fig. 1) need to be integrated, in which an AAD algorithm is combined with a reliable and low-latency speaker separation algorithm, a miniaturized EEG sensor system, and a smart gain control system.

Despite the many challenges ahead, the application of neuro-steered hearing devices as a neurorehabilitative assistive device has shown to be within reach, having the potential to substantially improve the functionality and user-acceptance of future generations of hearing devices.

POP-OUT BOXES

Pop-out box 1: Experiment details

Data: The characteristics of both datasets are summarized in the following table:

Attribute	Das-2015 [20]	Fuglsang-2018 [21]
Number of subjects	16	18
Amount of data (per subject)	72 min	50 min
EEG system	64-channel Biosemi	64-channel Biosemi
Speakers	male & male	male & female
Azimuth direction sources	$\pm 90^{\circ}$	$\pm 60^{\circ}$
Acoustic room condition	dichotic and HRTF-filtered in anechoic room	HRTF-filtered in anechoic, mildly, and highly reverberant room

Speech envelope extraction: The individual speech signals are passed through a gammatone filterbank, which roughly approximates the spectral decomposition as performed by the human auditory system. Per subband, the audio envelopes are extracted and their dynamic range is compressed using a powerlaw operation with exponent 0.6, after which the subband envelopes are summed into a single broadband envelope [30].

Frequency range: For computational efficiency, the speech envelopes as well as the EEG signals are both downsampled to $f_s = 64\,\mathrm{Hz}$, and bandpass filtered between 1–32 Hz [8]–[10]. For the linear algorithms, this was further reduced to $f_s = 20\,\mathrm{Hz}$ and 1–9 Hz in order to be able to reduce the number of parameters in the spatio-temporal decoders (linear stimulus reconstruction methods have been demonstrated to not exploit information above $9\,\mathrm{Hz}$ [30]).

Hyperparameter settings: The decoder lengths and CNN kernel lengths are set as in the original papers. For all linear methods, this is $250\,\mathrm{ms}$, for NN-SR $420\,\mathrm{ms}$, for CNN-loc $130\,\mathrm{ms}$, and for CNN-sim $30\,\mathrm{ms}$ (first layer) and $10\,\mathrm{ms}$ (second layer). For CCA, $1.25\,\mathrm{s}$

is chosen as the encoder length. The full set of 64 channels are used in all algorithms, except for MMSE-adap-lasso, where the same 28 channels as in [6] are chosen to reduce the number of parameters (since the decoder is estimated on much less data). The regularization parameters are cross-validated using 10 values in the range $[10^{-6}, 0]$. For CCA, it turned out that retaining all PCA components for both datasets is optimal.

Pop-out box 2: Details on cross-validation procedure

Two-stage cross-validation: The different algorithms are evaluated via a two-stage cross-validation (CV) procedure applied per subject and decision window length. The AAD accuracy is determined via an outer leave-one-segment-out CV (LOSO-CV) loop. Per outer fold, the optimal hyperparameter is determined via an inner ten-fold CV loop on the training set of the outer loop. The length of each left-out segment in the outer loop is chosen equal to $60\,\mathrm{s}$, which is split into smaller disjoint decision windows. For example, for a decision window length of $30\,\mathrm{s}$, each left-out segment results in two decisions. Additional details per AAD algorithm are provided in the following table (standard CV corresponds to training on all but one segment, testing on the left-out segment):

Method	**Outer LOSO-CV loop**	**Inner 10-CV loop**
MMSE-avgcorr-ridge/lasso	standard	optimization of λ (independent of τ, tuned based on largest value of τ)
MMSE-avgdec-ridge/lasso	training data of each fold is split into windows of the same size as τ. A different decoder is estimated in each of these subwindows and the decoders are averaged across all training folds (similar to [3])	optimization of λ (re-optimized for τ due to the dependency of the training procedure on τ)
CCA	standard, additional LOSO-CV loop to train and test LDA classifier	optimization of the number of canonical correlation coefficients J as input for LDA (re-optimized for each τ)
MMSE-adap-lasso	optimization of λ per τ and fold by taking hyperparameter with highest accuracy on training fold	/
NN-SR	standard	/
CNN-loc	LOSpO-CV instead of LOSO-CV, training *and* testing redone for τ	/
CNN-sim	standard, training *and* testing redone for τ	/

Overfitting to speakers: The CNN-loc algorithm has been shown to be prone to overfitting to speakers in the training set, thus showing overoptimistic performance when using the LOSO-CV method, where the test set always contains a speaker that is also present in the

training set [10]. Instead, we use the leave-one-speaker-out CV (LOSpO-CV) method for this algorithm, as explained in [10]. For the linear methods we use the standard LOSO-CV as these do not exhibit such overfitting. The latter is validated by performing 100 runs per subject, with in each run another random CV split (using the same amount of folds as for LOSpO-CV). We then tested whether the LOSpO-CV performance significantly differs from the median of this empirical distribution (i.e., the median over all random splits) over all subjects. For the CCA method, which has most degrees of freedom to overfit, the difference between the LOSpO-CV and median random-CV accuracy is less than 1% on 20s decision windows, and a paired Wilcoxon signed-rank test (over subjects) shows no significant difference ($W = 85, n = 16, p = 0.38$), indicating that there is no significant overfitting effect.

REFERENCES

[1] N. Mesgarani and E. F. Chang, "Selective cortical representation of attended speaker in multi-talker speech perception," *Nature*, vol. 485, no. 7397, pp. 233–236, 2012.

[2] N. Ding and J. Z. Simon, "Emergence of neural encoding of auditory objects while listening to competing speakers," *Proc. Natl. Acad. Sci.*, vol. 109, no. 29, pp. 11 854–11 859, 2012.

[3] J. A. O'Sullivan *et al.*, "Attentional Selection in a Cocktail Party Environment Can Be Decoded from Single-Trial EEG," *Cereb. Cortex*, vol. 25, no. 7, pp. 1697–1706, 2014.

[4] W. Biesmans *et al.*, "Auditory-inspired speech envelope extraction methods for improved EEG-based auditory attention detection in a cocktail party scenario," *IEEE Trans. Neural Syst. Rehabil. Eng.*, vol. 25, no. 5, pp. 402–412, 2017.

[5] E. Alickovic *et al.*, "A Tutorial on Auditory Attention Identification Methods," *Front. Neurosci.*, vol. 13, p. 153, 2019.

[6] S. Miran *et al.*, "Real-Time Tracking of Selective Auditory Attention from M/EEG: A Bayesian Filtering Approach," *Front. Neurosci.*, vol. 12, p. 262, 2018.

[7] A. de Cheveigné *et al.*, "Decoding the auditory brain with canonical component analysis," *NeuroImage*, vol. 172, pp. 206–216, 2018.

[8] T. de Taillez *et al.*, "Machine learning for decoding listeners attention from electroencephalography evoked by continuous speech," *Eur. J. Neurosci.*, 2017.

[9] G. Ciccarelli *et al.*, "Comparison of Two-Talker Attention Decoding from EEG with Nonlinear Neural Networks and Linear Methods," *Sci Rep*, vol. 9, no. 1, p. 11538, 2019.

[10] S. Vandecappelle *et al.*, "EEG-based detection of the locus of auditory attention with convolutional neural networks," *bioRxiv*, 2020. [Online]. Available: https://www.biorxiv.org/content/early/2020/02/27/475673

[11] S. Van Eyndhoven *et al.*, "EEG-Informed Attended Speaker Extraction From Recorded Speech Mixtures With Application in Neuro-Steered Hearing Prostheses," *IEEE Trans. Biomed. Eng.*, vol. 64, no. 5, pp. 1045–1056, 2017.

[12] J. OSullivan *et al.*, "Neural decoding of attentional selection in multi-speaker environments without access to clean sources," *J. Neural Eng.*, vol. 14, no. 5, p. 056001, 2017.

[13] C. Han *et al.*, "Speaker-independent auditory attention decoding without access to clean speech sources," *Sci. Adv.*, vol. 5, no. 5, pp. 1–12, 2019.

[14] W. Pu *et al.*, "A Joint Auditory Attention Decoding and Adaptive Binaural Beamforming Algorithm for Hearing Devices," in *Proc. IEEE Int. Conf. Acoust. Speech and Signal Process.*, 2019, pp. 311–315.

[15] A. Aroudi and S. Doclo, "Cognitive-driven binaural beamforming using EEG-based auditory attention decoding," *IEEE/ACM Trans. Audio, Speech, Language Process.*, vol. 28, pp. 862–875, 2020.

[16] S. Debener *et al.*, "Unobtrusive ambulatory EEG using a smartphone and flexible printed electrodes around the ear," *Sci Rep*, vol. 5, p. 16743, 2015.

[17] S. L. Kappel *et al.*, "Dry-Contact Electrode Ear-EEG," *IEEE Trans. Biomed. Eng.*, vol. 66, no. 1, pp. 150–158, 2019.

[18] B. Mirkovic *et al.*, "Target Speaker Detection with Concealed EEG Around the Ear," *Front. Neurosci.*, vol. 10, p. 349, 2016.

[19] A. M. Narayanan and A. Bertrand, "Analysis of miniaturization effects and channel selection strategies for EEG sensor networks with application to auditory attention detection," *IEEE Trans. Biomed. Eng.*, vol. 67, no. 1, pp. 234–244, 2020.

[20] N. Das *et al.*, "Auditory Attention Detection Dataset KULeuven," Zenodo, 2019. [Online]. Available: https://doi.org/10.5281/zenodo.3377911

[21] S. A. Fuglsang *et al.*, "EEG and audio dataset for auditory attention decoding," Zenodo, 2018. [Online]. Available: https://doi.org/10.5281/zenodo.1199011

[22] D. D. E. Wong *et al.*, "A Comparison of Regularization Methods in Forward and Backward Models for Auditory Attention Decoding," *Front. Neurosci.*, vol. 12, p. 531, 2018.

[23] J. P. Dmochowski *et al.*, "Extracting multidimensional stimulus-response correlations using hybrid encoding-decoding of neural activity," *NeuroImage*, vol. 180, pp. 134–146, 2018.

[24] S. Geirnaert *et al.*, "An Interpretable Performance Metric for Auditory Attention Decoding Algorithms in a Context of Neuro-Steered Gain Control," *IEEE Trans. Neural Syst. Rehabil. Eng.*, vol. 28, no. 1, pp. 307–317, 2020.

[25] T. Gerkmann *et al.*, "Phase processing for single-channel speech enhancement: History and recent advances," *IEEE Signal Process. Mag.*, vol. 32, no. 2, pp. 55–66, 2015.

[26] S. Gannot *et al.*, "A Consolidated Perspective on Multimicrophone Speech Enhancement and Source Separation," *IEEE/ACM Trans. Audio, Speech, Language Process.*, vol. 25, no. 4, pp. 692–730, 2017.

[27] Y. Luo and N. Mesgarani, "Conv-TasNet: Surpassing Ideal Time-Frequency Magnitude Masking for Speech Separation," *IEEE/ACM Trans. Audio, Speech, Language Process.*, vol. 27, no. 8, pp. 1256–1266, 2019.

[28] N. Das *et al.*, "Linear versus deep learning methods for noisy speech separation for EEG-informed attention decoding," *J. Neural Eng.*, 2020.

[29] S. A. Fuglsang *et al.*, "Effects of Sensorineural Hearing Loss on Cortical Synchronization to Competing Speech during Selective Attention," *J. Neurosci.*, vol. 40, no. 12, pp. 2562–2572, 2020.

[30] N. Das *et al.*, "The effect of head-related filtering and ear-specific decoding bias on auditory attention detection," *J. Neural Eng.*, vol. 13, no. 5, p. 056014, 2016.